Controlling the Functionality of Cytochrome c_1 Redox Potentials in the *Rhodobacter capsulatus* bc_1 Complex through Disulfide Anchoring of a Loop and a β-Branched Amino Acid near the Heme-Ligating Methionine†

Artur Osyczka,*,‡ P. Leslie Dutton,‡ Christopher C. Moser,‡ Elisabeth Darrouzet,§,|| and Fevzi Daldal§

The Johnson Research Foundation, Department of Biochemistry and Biophysics, and Department of Biology, Plant Science Institute, University of Pennsylvania, Philadelphia, Pennsylvania 19104

Received August 7, 2001; Revised Manuscript Received September 26, 2001

ABSTRACT: The cytochrome c_1 subunit of the ubihydroquinone:cytochrome *c* oxidoreductase (bc_1 complex) contains a single heme group covalently attached to the polypeptide via thioether bonds of two conserved cysteine residues. In the photosynthetic bacterium *Rhodobacter* (*Rba.*) *capsulatus*, cytochrome c_1 contains two additional cysteines, C144 and C167. Site-directed mutagenesis reveals a disulfide bond (rare in monoheme *c*-type cytochromes) anchoring C144 to C167, which is in the middle of an 18 amino acid loop that is present in some bacterial cytochromes c_1 but absent in higher organisms. Both single and double Cys to Ala substitutions drastically lower the +320 mV redox potential of the native form to below 0 mV, yielding nonfunctional cytochrome bc_1. In sharp contrast to the native protein, mutant cytochrome c_1 binds carbon monoxide (CO) in the reduced form, indicating an opening of the heme environment that is correlated with the drop in potential. In revertants, loss of the disulfide bond is remediated uniquely by insertion of a β-branched amino acid two residues away from the heme-ligating methionine 183, identifying the pattern βXM, naturally common in many other high-potential cytochromes *c*. Despite the unrepaired disulfide bond, the βXM revertants are no longer vulnerable to CO binding and restore function by raising the redox potential to +227 mV, which is remarkably close to the value of the βXM containing but loop-free mitochondrial cytochrome c_1. The disulfide anchored loop and βXM motifs appear to be two independent but nonadditive strategies to control the integrity of the heme-binding pocket and raise cytochrome *c* midpoint potentials.

The cytochrome bc_1 complexes play the role of transmembrane proton pumps in mitochondrial and bacterial electron transfer chains. A catalytic core of all cytochrome bc_1 complexes is formed by the three subunits that embed a total of four redox-active prosthetic groups and provide two distinct sites for binding quinone/quinol molecules. The four redox-active centers include a single *c*-type heme in the cytochrome c_1 subunit, a [2Fe2S] iron−sulfur cluster in the Fe-S subunit, and two *b*-type hemes, b_L and b_H, in the cytochrome *b* subunit. These redox centers provide the electron transfer frame for ubiquinone redox reactions at the Q_o site and the Q_i site acting to promote the translocation of protons across the membrane (for recent reviews see refs *1*−*3*).

A topographic arrangement of the subunits, predicted through biochemical studies and site-directed mutagenesis (*4*−*7*) and visualized by recently determined crystal structures of mitochondrial bc_1 complexes (*8*−*11*), shows that the cytochrome *b* subunit is almost entirely embedded in the membrane. In contrast, both cytochrome c_1 and the Fe-S subunit assemble as extrinsic, water-soluble domains anchored to the membrane through a hydrophobic α-helical tail formed at the respective C- or N-terminus of the cytochrome c_1 or the Fe-S subunit polypeptides. A long-range movement of the head domain of the Fe-S subunit has recently been postulated as a key feature securing the functionally critical bifurcation of electron transfer at the Q_o site (reviewed in ref *12*).

Cytochrome c_1 both structurally and functionally links the cytochrome bc_1 complex with its physiological redox partners, soluble or membrane-attached cytochromes *c* or soluble high-potential iron−sulfur proteins (HiPIPs). Cytochrome c_1 provides a docking site for these proteins on its surface at the membrane−aqueous interface and is oxidized by them. In turn, the oxidized cytochrome c_1 acts to oxidize the [2Fe2S] cluster, which then moves to the Q_o site.

The cytochrome c_1 subunit is, so far, the least studied catalytic subunit of the cytochrome bc_1 complex. Nevertheless, several structure−function relationships of this protein have been elucidated. It is clear that its extrinsic domain shares many of the electrochemical and structural properties of class I *c*-type cytochromes. It contains the consensus

† This work was supported by U.S. Public Health Service Grants GM-27309 to P.L.D. and GM-38237 to F.D.

* To whom correspondence should be addressed at 1004 Stellar-Chance Laboratories, Department of Biochemistry and Biophysics, University of Pennsylvania, Philadelphia, PA 19104-6059. Phone: 215-898-8699. Fax: 215-573-2235. E-mail: osyczkaa@mail.med.upenn.edu.

‡ The Johnson Research Foundation and the Department of Biochemistry and Biophysics.

§ Department of Biology.

|| Current address: Service de Biochimie Post-génomique et Toxicologie Nucléaire, DIEP, DSV, CEA VALRHO, 30207 Bagnols sur Cèze, France.

10.1021/bi011630w CCC: $20.00
Published on Web 11/08/2001

heme-binding motif (CXXCH) located close to the N-terminus of the polypeptide that provides sites for covalent attachment of the heme group (cysteines) and fifth axial ligation to the heme iron (histidine). It also contains the invariant methionine residue present near the C-terminus that acts as the sixth axial ligand to the heme iron. These two fundamental characteristics of heme ligation are complemented by a specific alignment of secondary structural elements, which shows high similarity to the basic folding pattern of Ambler's class I cytochromes. In particular, the helical segments, which are conserved in class I cytochromes (α1, α3, and α5), are present in cytochrome c_1 and occupy the same positions relative to each other and the heme plane (*9, 10*). This structural arrangement orients the heme inside a hydrophobic pocket in a highly specific manner (with the CD edge of the heme group exposed at the front face that encounters and interacts with its soluble redox partner) providing the environment that, added to the His-Met ligation, somehow defines its electrochemical functionality and establishes highly electropositive redox midpoint potential. Just how the structure establishes the potential has been the subject of numerous discussions (as examples see refs *13*−*19*).

Cytochrome c_1 has also some distinguishing characteristics that are not present in other cytochromes *c*. These represent mainly the results of structure−function-related insertions or deletions in the loop regions. A long N-terminal extension before helix α1 interacts with the hinge protein in mitochondrial cytochrome bc_1 complexes. A long insertion between the heme binding motif CXXCH and helix α3 includes a region implicated in cytochrome *c* binding (*20, 21*) and the contact between two cytochromes c_1 in the dimeric form of the complex. The insertion between the sixth heme ligand and helix α5 contains another portion of the cytochrome *c* binding site (*22*). On the other hand, the shortening of the loop that precedes helix α3 leaves the heme propionate edge exposed to the surface suitable for electron transfer from the [2Fe2Se] cluster (in cytochrome *c* this edge remains buried within the protein).

Some bacterial cytochromes c_1 have an additional insertion preceding the sixth heme ligand which is not present in the sequences of cytochromes c_1 of higher organisms (see Figure 1). Since the crystal structures of bacterial cytochrome bc_1 complex are currently undetermined, the 3D orientation of the insertion remains unknown. The present investigation examines the structural and functional properties of this region in cytochrome c_1 of the phototrophic bacterium *Rhodobacter* (*Rba.*)[1] *capsulatus*. We observe that the correct folding of this extra loop requires a presence of a disulfide bridge formed by two non-heme-binding cysteine residues of cytochrome c_1, Cys-144 and Cys-167, in the sequence located between the heme-binding domain and the C-terminus of the polypeptide. A genetic elimination of the bridge alters the structure of the heme-binding pocket, dropping the redox potential to nonfunctional levels consistent with an increase in the pocket dielectric or exposure to solvent. We also observe that the structural and functional impairments caused by the lack of the bridge in cytochrome c_1 can be reverted via second-site suppressor mutations that occur outside the loop region but on the same polypeptide segment closer to the heme-ligating methionine. This site-directed mutagenesis and reversion in *Rba. capsulatus* cytochrome c_1 provide a dynamic illustration of the two basic protein structural strategies that have previously been implicated in setting the high potentials of *c*-type cytochromes (*17*).

EXPERIMENTAL PROCEDURES

Preparation of Mutated Cytochrome bc_1 Complexes. Rba. capsulatus strains with mutated bc_1 complexes were generated as described previously (*23*). The mutations were constructed by site-directed mutagenesis using the QuikChange system from Stratagene and the plasmid pPET1 [a derivative of pBR322 containing a wild-type copy of *petABC* (*23*)] as the template DNA. The following mutagenic primers were used to introduce single mutations (F and R denote forward and reverse primers, respectively): 5′-GAA AAC CCG GAA GCC GCC CCG GAA GGG ATC G-3′ (C144A-F), 5′-CCT TCC GGG GCG GCT TCC GGG TTT TCT TCG-3′ (C144A-R); 5′-TGC CGG ACA CCG CCA AGG ACG C-3′ (C167A-F), 5′-GTC CTT GGC GGT GTC CGG CAC G-3′ (C167A-R); 5′-GAT CGA TGG CCG CTA CTA CAA CAA G-3′ (Y152R-F), 5′-GTT GTA GTA GCG GCC ATC GAT CCC TTC-3′ (Y152R-R). A template with the double mutation C144A/C167A was constructed by an addition of a single mutation C167A to the plasmid pPET1 containing the mutation C144A. A similar method was adopted to construct the double mutant Y152R/C167A (a single mutation Y152R was added to the template containing C167A). After sequencing, the appropriate DNA fragments bearing the desired mutation and no other mutations were exchanged with their wild-type counterparts in pMTS1 [the expression vector containing a copy of *petABC* and a kanamycin resistance cartridge (*24*)] using the restriction enzymes *Sfu*I/*Xma*I and *Stu*I. The mutated variants of pMTS1 were then introduced into MT-RBC1 strain [*petABC*-operon deletion background (*23*)] via triparental crosses as described previously (*23*). The presence of engineered mutations was confirmed by sequencing the plasmid DNA isolated from the mutated *Rba. capsulatus* strains.

Spontaneous Ps^+ revertants of the C144A, C167A, and C144A/C167A mutants were obtained on MPYE plates containing kanamycin over several days of incubation under selective photosynthetic conditions. The Ps^+ colonies were then propagated extensively under these growth conditions, and their plasmid DNA was extracted and sequenced to determine the location and nature of the suppressor mutations. In each case the entire *petC* gene was subjected to the DNA sequence analysis, and only the single second-site reversions were found. The *Hin*dIII/*Xma*I fragment containing the cysteine substitutions (C144A/C167A) and the second-site reversion (A181T) obtained from pMTS1 of one of the revertant strain was exchanged with its counterpart on pMTS1 carrying the wild-type copy of the *petABC* operon. The plasmid so obtained was conjugated into the *Rba. capsulatus* MT-RBC1 strain to obtain the C144A/

[1] Abbreviations: bc_1 complex, ubihydroquinone:cytochrome *c* oxidoreductase; Ps^+, photosynthesis proficient; Ps^-, photosynthesis incompetent; E_m, redox midpoint potential; E_h, ambient redox potential; SHE, standard hydrogen electrode; SDS, sodium dodecyl sulfate; SDS−PAGE, sodium dodecyl sulfate−polyacrylamide gel electrophoresis; DTT, dithiothreitol; TMBZ, tertamethylbenzidine; DBH_2, 2,3-dimethoxy-5-decyl-6-methyl-1,4-benzohydroquinone; MOPS, 3-(*N*-morpholino)-propanesulfonic acid; wt, wild type; *Rba.*, *Rhodobacter*.

C167A/A181T mutant that expressed the cytochrome bc_1 complex containing the reversion used for further biochemical analysis.

Analysis of the Mutants. Chromatophore membranes and purified bc_1 complexes were prepared as described in refs *23* and *24*. Sodium dodecyl sulfate−polyacrylamide gel electrophoresis (SDS−PAGE) was performed according to Laemmli (*25*) using a 15% linear separating gel. The gels were stained with Coomassie blue for proteins or with tetramethylbenzidine (TMBZ) for covalently attached hemes (*26*). The immunoblot analysis was performed on Immobilon P-membranes (Millipore, Inc.) using polyclonal antibodies raised against the cytochrome c_1 subunit of the *Rba. capsulatus* bc_1 complex (*23*). Horseradish peroxidase-conjugated anti-rabbit secondary antibodies (Bio-Rad) and metal ion enhanced diaminobenzidine (DAB) staining were used to detect the immune complexes. Steady-state enzymatic activity of the cytochrome bc_1 complex was assayed by measuring DBH_2-dependent reduction of mitochondrial horse cytochrome *c* as described in ref *23*, and the rate of cytochrome *c* reduction was related to the molar content of cytochrome c_1. Optical spectra were recorded on a Perkin-Elmer UV/vis spectrophotometer (Lambda 20) fitted with an anaerobic redox cuvette when necessary. The difference spectra for *c*- and *b*-type cytochromes were obtained with samples that were first oxidized by an addition of potassium ferricyanide (to a final concentration of 20 μM) and then reduced by using either sodium ascorbate (added to a final concentration of 2 mM) or a minimal amount of solid, fresh sodium dithionite. Chemical oxidation−reduction midpoint potential titrations of purified complexes were performed as described in ref *27*. The titrations were performed in 50 mM MOPS (pH 7.0) containing 100 mM NaCl and redox mediators tetrachlorohyroquinone, 2,3,5,6-tetramethyl-1,4-phenylenediamine, 1,2-naphthoquinone-4-sulfonate, 1,2-naphthoquinone, phenazine ethosulfate, phenazine methosulfate, duroquinone, pyocyanine, 2-hydroxy-1,4-naphthoquinone, and anthraquinone-2-sulfonate at concentrations of 15−30 μM. The optical changes that accompanied redox potential change were recorded in the α-band region (500−600 nm) or in the Soret region (400−450 nm), and the E_m values were determined by fitting the data to a single $n = 1$ Nernst expression. The CO binding experiments were performed at room temperature using a sealed anaerobic cuvette. Purified, intact bc_1 complexes dissolved in 50 mM Tris-HCl (pH 7.5) containing 100 mM NaCl were first reduced by exchanging of air with argon followed by an anaerobic addition of sodium dithionite. The CO was then introduced to the samples by short bubbling. The reduced + CO *minus* reduced spectra were analyzed.

Factor Xa Enzymatic Proteolysis. Purified bc_1 complexes (at concentration of 10 μM in 50 mM Tris-HCl, 100 mM NaCl, pH 8.0) were incubated at 50 °C for 10 min in the presence of 0.01% SDS. Iodoacetamide was then added to a final concentration of 10 mM, and samples were incubated for 10 min at room temperature. After this treatment, factor Xa protease (New England Biolabs) was added at a w/w ratio of 1% the amount of the cytochrome bc_1 complex, and the reaction was carried out for 16 h at room temperature. After the protease digestion, the samples were mixed with the SDS−PAGE loading buffer, incubated at 60 °C for 5 min in the presence of 100 mM DTT or in the absence of any reducing agent, and subjected to SDS−PAGE/immunoblot analysis as described above.

The treatment with factor Xa (see above) was carried out in the presence of blocking reagent (iodoacetamide) to exclude the possibility of the formation of intramolecular disulfide linkages during the cleavage. It should be added, however, that this concern proved to be unfounded since samples not treated with iodoacetamide exhibited the same SDS−PAGE profiles of the cleavage products as those samples treated with this reagent.

Evaluation of the Oxidation−Reduction Properties of the Disulfide Bridge in Cytochrome c_1 Using a Factor Xa Cleavage Assay. The purified bc_1 complex containing the mutation Y152R was digested with factor Xa as described above. The cleavage was stopped by addition of dansyl-Glu-Gly-Arg chloromethyl ketone (Calbiochem) to a final concentration of 3 μM. This mixture was subjected to a reductive potentiometric titration in the presence of the following redox mediators: 2-hydroxy-1,4-naphthoquinone, anthraquinone-2-sulfonate, benzyl viologen, methyl viologen, and 1,1-trimethylene-2,2-bipyridyl salt. Each mediator was used at a concentration of 12.5 μM, and the titration was carried out using standard redox potentiometric procedures (*27*). For the potentials lower than −480 mV, titanium(III) citrate (*28*) was used as a reductant instead of sodium dithionite. At each specific potential, an aliquot of 30 μL was withdrawn (after 25 min equilibration time) and mixed with 3 μL of 125 mM iodoacetamide. The samples were then incubated at 60 °C for 5 min and subjected to SDS−PAGE under nonreducing conditions.

RESULTS

Replacement of the Non-Heme-Binding Cysteine Residues in Cytochrome c_1. Rba. capsulatus cytochrome c_1 contains two cysteine residues (C144 and C167) that do not participate in the covalent attachment of the heme (Figure 1). Using site-directed mutagenesis, these residues have been changed to Ala residues by constructing two single mutants, C144A and C167A, and a double mutant, C144A/C167A. The properties of mutants are summarized in Table 1.

The SDS−PAGE and TMBZ heme staining analysis of the bc_1 complexes isolated from the mutated strains revealed that in all cases the expressed bc_1 complexes contain the three subunits assembled correctly and the heme group covalently attached to cytochrome c_1 (Figure 2). These bc_1 complexes, however, appear to be functionally impaired, as indicated by the Ps^- phenotype of the cells. Direct measurement of steady-state activity confirmed this observation: the bc_1 complexes isolated from all three mutants show greatly reduced DBH_2 activity compared to the bc_1 complex isolated from the wild-type cells (Table 1).

Optical difference spectra of isolated bc_1 complexes shown in Figure 3a−d reveal that the deleterious effect of cysteine substitutions on function is accompanied by the changes in the redox properties of cytochrome c_1. The spectrum of the wild-type bc_1 complex is characterized by the presence of both ascorbate and dithionite reducible components (Figure 3a). The ascorbate-reducible component at 552 nm reflects the reduced state of cytochrome c_1, while the dithionite-reducible components include cytochromes b_L and b_H in addition to cytochrome c_1 (*29*). In contrast, the spectra of

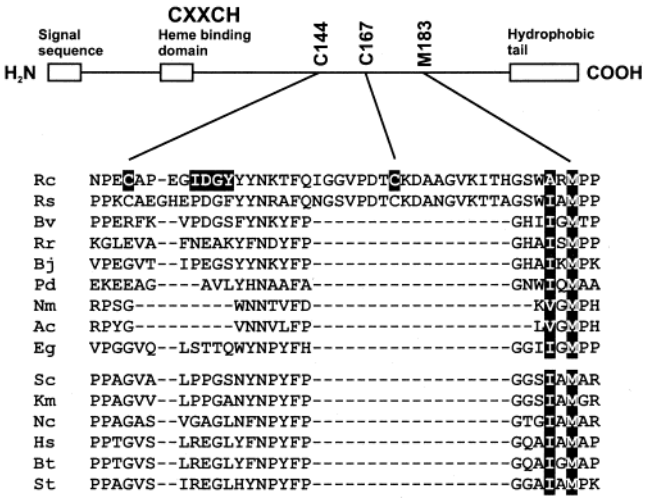

FIGURE 1: Schematic diagram of the primary organization of the cytochrome c_1 polypeptide (top) and partial sequence comparison of various cytochromes c_1 (bottom): Rc, *Rhodobacter capsulatus*; Rs, *Rhodobacter sphaeroides*; Bv, *Blastochloris viridis*; Rr, *Rhodospirillum rubrum*; Bj, *Bradyrhizobium japonicum*; Pd, *Paracoccus denitrificans*; Nm, *Neisseria meningitidis*; Ac, *Allochromatium vinosum*; Eg, *Euglena gracilis*; Sc, *Saccharomyces cerevisiae*; Km, *Kluyveromyces marxianus*; Nc, *Neurospora crassa*; Hs, *Homo sapiens*; Bt, *Bos taurus*; St, *Solanum tuberosum*. The following residues are shaded: the non-heme-binding cysteine residues of *Rba. capsulatus* (C144 and C167), the conserved sixth axial ligand to the heme iron (M183 in *Rba. capsulatus*), the position of second-site reversions in cysteine mutants (A181 in *Rba. capsulatus*), and the IDGY motif that was converted into a factor Xa cleavage site IDGR in the Y152R and Y152R/C167A mutants.

Table 1: Mutagenesis of Non-Heme-Binding Cysteine Residues in *Rba. capsulatus* Cytochrome c_1

mutation	photosynthetic growth[a]	enzymatic activity (s^{-1})[b]	properties of cytochrome c_1 heme in the bc_1 complex		reversion to Ps^+[e]
			E_{m7} (mV)[c]	CO binding[d]	
wild type	+	92	+320	−	na[f]
C144A	−[g]	1	−58	+	A181T
C167A	−	1.3	−49	+	A181T
C144A/C167A	−	1.2	−76	+	A181T A181V
C144A/C167A/A181T	+	64	+227	−	na

[a] (+) and (−) indicate the ability to grow photosynthetically on MPYE plates. [b] DBH_2 cyt *c* oxidoreductase activity was measured as described in Experimental Procedures and expressed as a turnover rate of cytochrome *c* reduction by purified bc_1 complexes. [c] Midpoint redox potential of cytochrome c_1 in isolated bc_1 complexes. [d] (+) and (−) indicate the ability of ferrocytochrome c_1 in isolated bc_1 complexes to bind carbon monoxide. [e] Spontaneous second-site suppressor mutations in cytochrome c_1 that restore photosynthetic activity of the cells. [f] Not applicable. [g] Ps^- phenotype was also obtained for the mutation C144S.

all three cysteine mutants show no ascorbate-reducible cytochrome c_1. Reduced cytochrome c_1 is seen only after dithionite reduction (shoulder at 553−554 nm) along with the reduction of cytochromes *b* (peak at 560 nm) (Figure 3b−d). The lack of ascorbate-reducible components in the cysteine mutants implies that the mutated bc_1 complexes no longer have the high-potential form of cytochrome c_1 characteristic of the wild-type complex. This immediately suggests that cytochrome c_1 in these mutants has dramatically lowered redox midpoint potentials with respect to the wild type.

The lowered values of redox potentials in the mutants were quantified by the redox potentiometric titrations (Figure 4). The titrations and accompanying spectral changes in the α-region confirm the presence of high-potential cytochrome c_1 in the wild-type bc_1 complex ($E_m = +320$ mV) (*29*) and the absence of any high-potential form (above +60 mV) of cytochrome c_1 in the mutants. More specifically, the mutated cytochromes c_1 titrate together with the *b*-hemes in a low range of potentials (below +60 mV). In this range of potentials the spectral contributions from the *c*- and *b*-hemes are best resolved in the Soret region where it has been shown that the reduction of low-potential forms of cytochrome c_1 contribute a shoulder at 420 nm clearly resolvable from the *b*-hemes (*30*). The profiles of this transition shown in Figure 4 reveal E_m values of −58, −49, and −76 mV for C144A, C167A, and C144A/C167A, respectively (Table 1). Thus, the cysteine substitutions decrease the reduction potential by more than 300 mV with respect to the wild type, an effect that readily can explain all of the observed growth and enzymatic defects of the mutants. Furthermore, the magnitude of the decrease suggests that the mutations might have altered the structure of the heme-binding pocket itself and consequently perturb the nature and/or strength of the ligand interaction with the heme iron. Such perturbation of heme proteins has a well-known effect of rendering the heme more prone to binding by exogenous ligand such as carbon monoxide, azide, or cyanide.

Figure 5 compares the wild-type and mutated bc_1 complexes in terms of their abilities to bind carbon monoxide. The difference spectra (dithionite reduced + CO *minus* dithionite reduced) of mutated bc_1 complexes show large transitions in the Soret region and smaller but significant transitions in the α-region (Figure 5b−d), in contrast to the wild type, which shows relatively small perturbations mainly in the Soret region (Figure 5a). The spectral characteristics of these transitions (a clear negative peak at 552−553 nm present in the mutant bc_1 complexes but absent in the wild type) are consistent with CO binding to the reduced cytochrome c_1 of the mutants but not to the wild type. They also reflect a minor residual portion of *b*-hemes that bind CO. (This latter effect is most probably an artifact resulting from the partial unfolding and denaturation of *b*-hemes during the isolation procedures. The ascorbate reduced + CO *minus* ascorbate reduced difference spectrum of the wild-type bc_1 complex shows no transitions, excluding the possibility that reduced cytochrome c_1 in the complex binds CO.) Furthermore, the spectra of C144A, C167A, and C144A/C167A (Figure 5b−d) are similar to that of the previously characterized mutant M183L in which the methionine axial ligand to the heme was replaced by leucine (Figure 5f). Since M183L has already been shown to bind CO with purified cytochrome c_1 preparations (*30*), this confirms our assignment and strengthens the notion that the cysteine mutations induce in cytochrome c_1 some alterations in the heme axial ligation.

Spontaneous Reversion of Cysteine Mutants to the Ps^+ Phenotype. Photosynthetically inactive strains carrying either single mutations C144A or C167A or the double mutation C144A/C167A, when incubated under photosynthetic conditions, revert spontaneously to the photosynthetically competent strains. The DNA sequence analysis of the revertant strains revealed that they retain the original cysteine substitutions and have a single second-site suppressor mutation. The

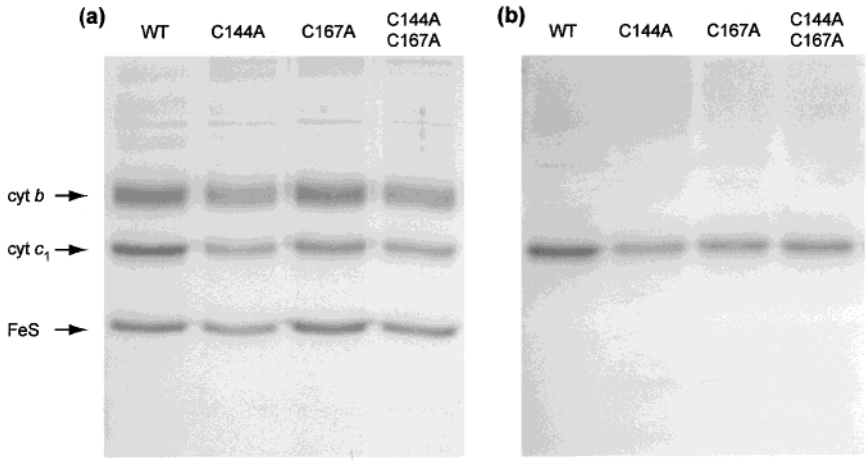

FIGURE 2: SDS−PAGE analysis of the cytochrome bc_1 complexes isolated from the wild-type and cytochrome c_1 cysteine mutants: C144A, C167A, and C144A/C167A. Samples of protein were incubated under reducing conditions at 60 °C for 5 min prior to the loading on 15% acrylamide gels. The gels were stained for proteins with Coomassie blue (a) and for heme with TMBZ (b).

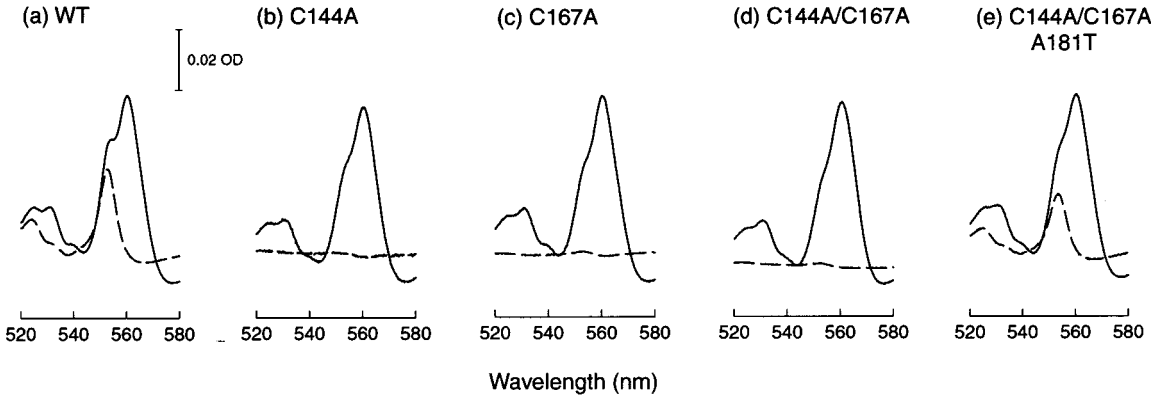

FIGURE 3: Optical redox difference spectra of the cytochrome bc_1 complexes isolated from wild type (a), single mutants C144A (b) and C167A (c), double mutant C144A/C167A (d), and triple mutant C144A/C167A/A181T (e). Spectra were obtained using samples of protein (1.5 μM) dissolved in 50 mM Tris-HCl (pH 8.0), containing 100 mM NaCl and 0.1 mg/mL dodecyl maltoside. Solid and dashed lines correspond to dithionite *minus* ferricyanide and ascorbate *minus* ferricyanide spectra, respectively.

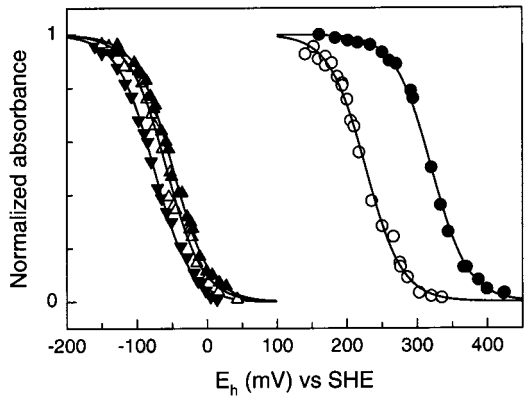

FIGURE 4: Redox midpoint potentials of cytochromes c_1 in the purified bc_1 complexes. Reductive dark equilibrium redox titrations were performed as described in Experimental Procedures. Plots: (●) wild type and (○) C144A/C167A/A181T monitored at 552−548 nm; (△) C144A, (▲) C167A, and (▼) C144A/C167A monitored at 420 nm. The data were fit to the Nernst equation for a one-electron couple. The E_m values obtained are listed in Table 1.

suppression, regardless of the position of original cysteine substitutions, is always located at the same position within the *petC* gene and in the polypeptide chain replaces A181 by another amino acid (Table 1). Of five clones analyzed for the reversion in the C144A/C167A mutant, four changed A181 to threonine and the fifth to valine. One clone analyzed for either C144A or C167A revealed A181T substitution. It is of note that these second-site suppressions occur in close proximity to the position occupied by the sixth axial ligand to the heme iron—M183 (Figure 1).

The difference absorption spectra of the bc_1 complex isolated from the mutant C144A/C167A/A181T (Figure 3e) reveal that A181T reversion, which restores the functionality of the complex, is accompanied by a raised midpoint potential of mutated cytochrome c_1. This is indicated by the reappearance of an ascorbate-reducible component in the spectrum. Similar spectra have been obtained for the mutant C167A/A181T (not shown).

The redox titration shows that the E_m value of cytochrome c_1 in the revertant mutant C144A/C167A/A181T has moved up substantially to a value of 227 mV (Figure 4) but remaining a significant 90 mV lower than the wild type. Nevertheless, this value is evidently high enough to support photosynthetic growth of the cells. Closer examination of the revertant for enzymatic activity (Table 1) and CO binding (Figure 5e) demonstrates that the return of the E_m value to 227 mV is accompanied by a return of much of the activity and a restoration of the heme ligation sufficient to prevent CO binding.

The observation that the effect of cysteine substitutions at positions 144 and 167 is naturally suppressed by the same

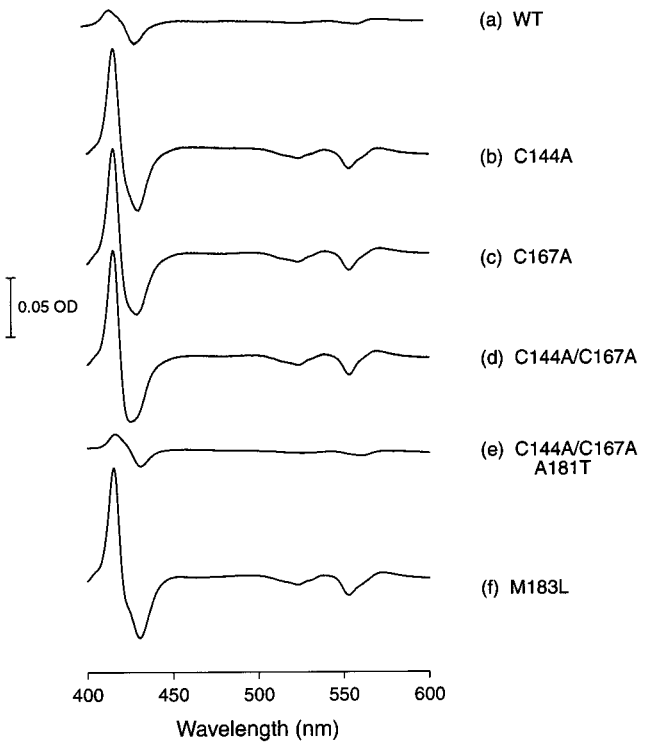

FIGURE 5: CO optical difference spectra (dithionite reduced + CO *minus* dithionite reduced) of the cytochrome bc_1 complexes isolated from wild type (a), single mutants C144A (b) and C167A (c), double mutant C144A/C167A (d), triple mutant C144A/C167A/A181T (e), and single mutant M183L (f). CO binding experiments were performed as described in Experimental Procedures with the samples containing 2 μM bc_1 complex.

second-site reversions at position 181 points toward an interesting possibility that C144 and C167 are structurally linked together and form a disulfide bond in the native structure.

Determination of the Presence of a Disulfide Bridge in Cytochrome c_1. When the amino acid sequence of a protein offers a unique proteolytic site situated in the region between the two cysteine residues, enzymatic proteolysis can be used to determine whether these two cysteines form a disulfide bridge. The approach relies on an assumption that if the bridge exists, the SDS−PAGE electrophoretic profile of the products of cleavage depends on the presence of reducing agents such as DTT. Thus in the absence of reducing agent, cleaved polypeptides linked together by the bridge will be expected to run as one polypeptide of larger size, whereas in the presence of reducing agent they should separate into two bands of smaller size.

Although the region between C144 and C167 in *Rba. capsulatus* cytochrome c_1 does not contain any full proteolytic site, it includes an "IDGY" motif, which can be converted to a site for factor Xa protease ("IDGR") by single amino acid substitution Y152R (see Figure 1). We have constructed two factor Xa "cleavable" mutants of cytochrome c_1 with the purpose of testing the presence of a disulfide bond between C144 and C167 in this protein. In the first mutant, the substitution Y152R is introduced into the wild-type sequence containing both C144 and C167 (a single mutant Y152R); the second one (a positive control) has the substitution Y152R introduced to the mutant without one cysteine (a double mutant Y152R/C167A). The mutation Y152R yields a photosynthetically competent strain producing the cytochrome bc_1 complex that has a wild-type spectra and electrochemical properties of high-potential cytochrome c_1 and a wild-type enzymatic activity (data not shown). This indicates that the Y152R mutation does not introduce major structural changes to the protein, allowing us to assume that the factor Xa proteolytic profiles obtained with this mutant (see below) will reflect the state of wild-type cytochrome c_1.

Figure 6 compares the electrophoretic profiles of the bc_1 complexes from wild-type, Y152R, and Y152R/C167A that were treated with factor Xa prior to the SDS−PAGE, in addition to the corresponding samples not treated with the enzyme. It can be seen that factor Xa does not cleave any of the subunits of the wild-type bc_1, consistent with a lack of sites for this enzyme in the whole sequence of the complex (Figure 6a,b, lanes 1 and 2). In contrast, the cleavage sites introduced by mutation in Y152R and Y152R/C167A are clearly recognized by the enzyme. This is indicated by the presence of two additional bands that appear at the expense of the cytochrome c_1 band in samples treated with DTT (Figure 6b, lanes 4 and 6). The estimated size of the bands, 12 and 18 kDa, agrees well with the size of polypeptides expected from the cleavage at the introduced site. In the corresponding samples not treated by any reducing agent, the cleaved peptides can only be seen in Y152R/C167A (Figure 6a, lane 6), while in Y152R, cytochrome c_1 still runs as a single band of unchanged size (Figure 6a, lane 4). Hence we find that the two cleaved parts are linked together, accounting for the observed SDS profile of Y152R only when both C144 and C167 are present. This provides the first convincing evidence that, in *Rba. capsulatus* cytochrome c_1, the two cysteines C144 and C167 are involved in the formation of a disulfide bridge, which, in light of the results obtained with the mutants neutralizing the thiols of those cysteines, appears to play a crucial role in securing the proper structure, spectral and electrochemical character, and functionality of the protein. The presence of the disulfide bond in this cytochrome appears also as the major structural difference between the catalytic core of *Rba. capsulatus* and mitochondrial cytochrome bc_1 complexes [the crystal structures of mitochondrial complexes do not show any disulfide-bonded cysteines in the cytochrome c_1 subunit (*8*−*11*)].

It should be added that an immunoblot with the use of antibodies against the cytochrome c_1 subunit confirmed the assignment of cleaved bands of 12 and 18 kDa as being parts of cytochrome c_1 (Figure 6c, lane 4). In addition, the immunoblot did not show any traces of cleaved products in Y152R not treated with DTT (Figure 6c, lane 2) which, given the higher sensitivity of Western blots over SDS−PAGE, indicates that in the isolated cytochrome bc_1 complex most probably the entire population of cytochrome c_1 contains the disulfide bond.

Oxidation−Reduction Properties of the Disulfide Bond. Although disulfides are redox-active centers and could conceivably participate in functional electron transfer reactions, the measure of redox potential values of these centers is quite challenging. In our system, however, the appearance of the cleaved peptides in the SDS−PAGE profile of the Y152R bc_1 complex digested by factor Xa is related to the redox state of the thiols forming the disulfide bond. Thus, quantitative monitoring of this process as a function of ambient redox potential should allow us to estimate at least

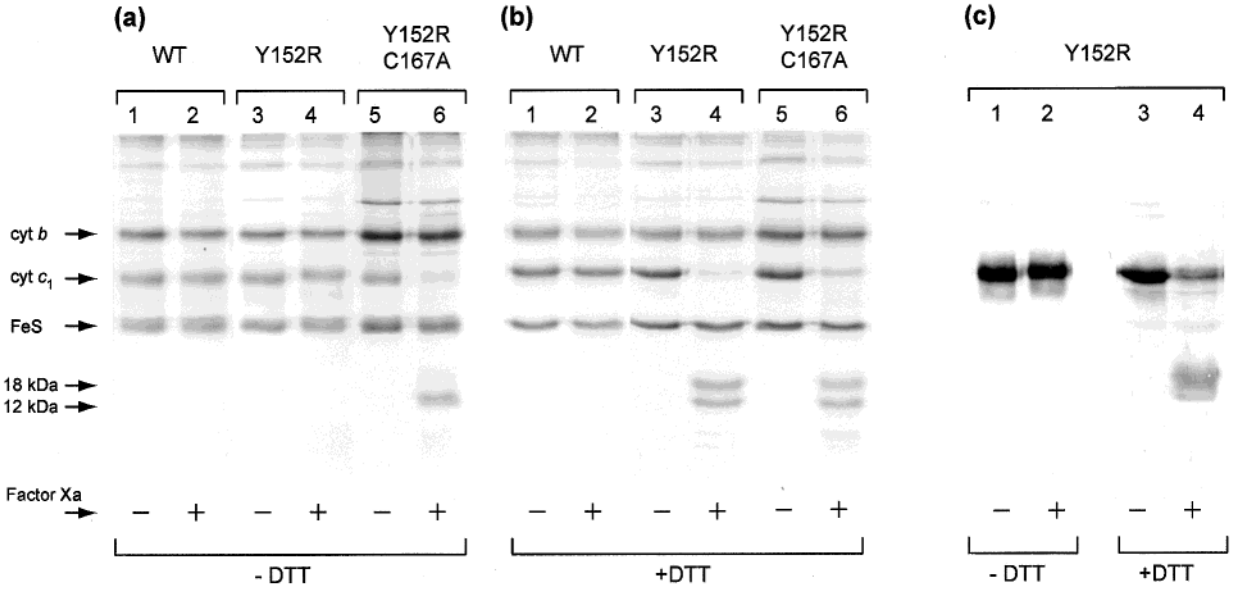

FIGURE 6: Determination of the presence of the disulfide bond in *Rba. capsulatus* cytochrome c_1 using a factor Xa cleavage assay. Panel a: SDS−PAGE profiles of the cytochrome bc_1 complexes isolated from the wild type and factor Xa-cleavable mutants (Y152R and Y152R/C167A). The samples were undigested (lanes 1, 3, and 5) or digested with factor Xa (lanes 2, 4, and 6) and incubated at 60 °C for 5 min in the absence of any reducing agent prior to the SDS−PAGE. The electrophoresis was carried out under nonreducing conditions, and the acrylamide gels (15%) were stained with Coomassie blue. The digestion with factor Xa was performed as described in Experimental Procedures. Panel b: Same as panel a except that the samples were incubated at 60 °C for 5 min in the presence of 100 mM DTT prior to the SDS−PAGE. Panel c: Immunoblot of Y152R using polyclonal antibodies against the cytochrome c_1 subunit. Lanes 1 and 2 of panel c correspond to lanes 3 and 4 of panel a, respectively. Lanes 3 and 4 of panel c correspond to lanes 3 and 4 of panel b, respectively.

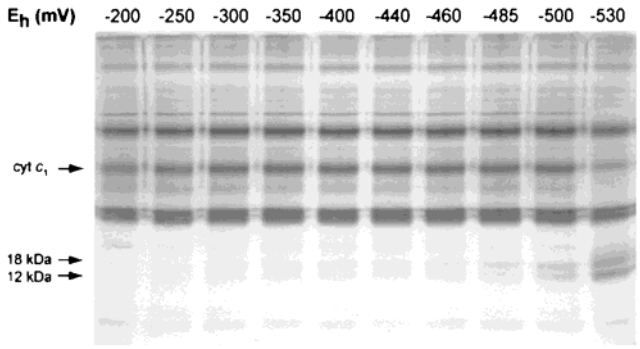

FIGURE 7: Evaluation of the oxidation−reduction properties of the disulfide bond in *Rba. capsulatus* cytochrome c_1 in the bc_1 complex using a factor Xa cleavage assay. The 15% acrylamide gel stained with Coomassie blue shows the SDS−PAGE profile of the Y152R mutant digested with factor Xa and poised at potentials indicated at the top of each line. The conditions for the enzymatic digestion and redox potentiometry are described in Experimental Procedures. Samples were incubated at 60 °C for 5 min in the absence of any reducing agent prior to the SDS−PAGE, and the electrophoresis was carried out under nonreducing conditions.

the range where the disulfide bond becomes susceptible to reduction, if not a reversible E_m for the disulfide/dithiol couple. The electrophoretic profiles obtained during such a redox titration shown in Figure 7 identify the approximate range of potentials at which the disulfide/dithiol exchange occurs. It can be seen that cleaved bands start to appear at potentials lower than −300 mV and their intensity increases with lowering the potential down to −530 mV. This very low redox potential range observed for the onset of the disulfide/dithiol exchange reveals the resistance of the disulfide bond to reduction and cleavage over a broad range of ambient potentials and down to strongly reducing potentials that are likely to be outside the physiological range.

DISCUSSION

Disulfide bonds are often viewed as a relatively simple strategy to increase protein stability, both in natural and in engineered systems (*31*, *32*). The vast majority of monoheme *c*-type cytochromes apparently have folding mechanisms that do not rely on cysteine bridges for conformational stability. However, we have demonstrated that *Rba. capsulatus* cytochrome c_1 is one of the few exceptions that contains a disulfide bond (for other exceptions see refs *33*−*36*). The disulfide anchors C144 to C167, which is in the middle of an 18 amino acid loop that is present in *Rhodobacter* cytochromes c_1 but absent in cytochromes *c* from higher organisms (Figure 1). Once C144 and C167 are oxidized to a disulfide, the low ambient potential required for reduction (Figure 7) makes the bond unlikely to participate in redox reactions and break under physiological conditions. When either C144 or C167 is changed to Ala, the mutant cytochromes c_1 are still equipped with heme and assemble with the other native subunits of the cytochrome bc_1 complex. However, the mutated bc_1 complex is virtually inactive; disruption of the disulfide bond dramatically lowers the redox potential of cytochrome by 380−400 mV so that it can no longer support the electron transfer between iron−sulfur protein and cytochrome c_2. Other possible effects may include structural changes that impede the formation of the reaction complex with soluble cytochrome c_2 or Rieske iron−sulfur protein.

In revertants, the loss of function was uniquely remediated by single amino acid substitutions that place a β-branched amino acid at position 181 (A181T, A181V), two residues away from the heme-ligating methionine M183, in the pattern βXM (Figure 1). This brought the E_m of cytochrome c_1 back to the high range of potentials (above +200 mV). Clearly, point mutations in the protein domain preceding M183 can

have very substantial, 6.6−8.8 kcal/mol, effects on heme redox potential in these cases without disrupting assembly. It may be significant that the domain of the sixth axial ligand (between helix α3 and α5) is comparatively mobile in the related soluble cytochromes *c* and c_2 (*37*−*40*) and has been identified as the last protein domain to fold (*41*). As the last fold, mutational effects in this domain may be conspicuous but relatively localized and focused.

Exposure to CO provides some insight into the effect of the mutations on the heme environment. Upon loss of the disulfide bridge and lowering of the redox potential, CO is admitted into the heme-binding pocket. Introduction of the β-branched amino acid at position 181 raises the potential and restores inaccessibility to CO, despite the fact that the disulfide is still disrupted. It is clear that mutants of the protein domain ranging from the heme-ligating M183 to at least C167 influence the strength of packing around the cytochrome c_1 heme which is normally responsible for promoting His-Met heme ligation and preventing access to other ligands, such as CO, water, or a second histidine. Furthermore, this domain has been shown to shift when related cytochromes *c* and c_2 are exposed to an excess of imidazole to displace the methionine ligand (*39*, *40*). Thus the drop in the redox potentials in the cytochrome c_1 mutants may represent a partial opening or weakening of the heme cleft, perhaps with an increased static or dynamic exposure of the heme to the external aqueous phase with possible charge compensating protons, generally raising the dielectric of the heme environment. All of these effects stabilize the oxidized form and, hence, lower the redox potential.

Besides raising the dielectric, the diminished structural integrity of the region around the heme pocket and loss of strength of the His-Met ligation may lead to an adventitious but favorable bis-His ligation using a free histidine in the structure. Bis-His ligated subpopulations have previously been observed in bacterial cytochromes c_1 when isolated from the cytochrome bc_1 complex (*42*) and suggested for sixth axial ligand mutants of *Rba. capsulatus* cytochrome c_1 (*30*, *43*). The redox potentials of cytochrome c_1 without the disulfide bridge are at the low limit of the range spanned by the large number of native His-Met ligated cytochromes *c* but well within the range of bis-His coordinated cytochromes *c* (see Figure 8). If the mutant is bis-His coordinated, the redox potential remains significantly higher than the values of imidazole-ligated porphyrins in aqueous solution, suggesting that the loosened heme-binding pocket would still retain some shielding from the external aqueous phase. However, without further spectroscopy, the question of whether the heme maintains the original His-Met coordination or adopts a bis-His coordination in a locally misfolded state cannot be decided. Nevertheless, H177 is only six residues away from M183 (Figure 1) and a likely candidate for alternative ligation. H177 could even play a physiological role as a normal folding intermediate of the *Rba. capsulatus* cytochrome c_1 analogous to bis-His ligation states implicated in folding pathways of mitochondrial cytochrome *c* (*41*, *44*).

The βXM reversion leaves the disulfide bridge unrepaired. This suggests that the disulfide anchoring of the extra loop and the βXM motif are independent and nonadditive strategies to control the integrity of the heme-binding pocket and raise the redox potential. Nonadditivity is supported by the fact that closely related *Rhodobacter sphaeroides* cytochrome

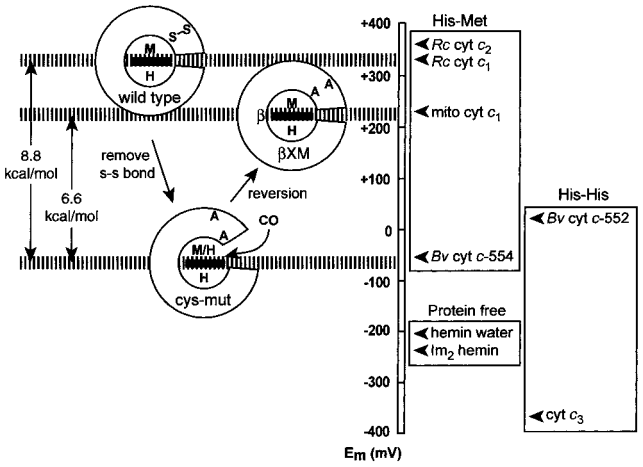

FIGURE 8: Schematic illustration of structural and redox potential changes of *Rba. capsulatus* (*Rc*) cytochrome (cyt) c_1 upon the mutational removal of the disulfide bond and the introduction of second-site reversions. Cytochromes c_1 potentials are compared to bisimidazole-ligated (Im_2) porphyrins and free hemin in aqueous solution (*51*) and other *c*-type cytochromes: *Desulfovibrio vulgaris* cytochrome c_3 (*52*), *c*-554 (4th) and *c*-552 (2nd) hemes of the tetraheme cytochrome subunit of *Blastochloris viridis* (*Bv*) RC (*53*), *Bos taurus* mitochondrial (mito) cytochrome c_1 (*54*), and *Rba. capsulatus* (*Rc*) cytochrome c_2 (*55*). The cysteine mutations (cys-mut) destabilize the reduced vs oxidized state by 8.8 kcal/mol compared to the wild type. If no ligand exchange takes place, this destabilization can be associated with heme site opening. If a His-Met to His-His ligation change is involved, about 3.6 kcal/mol of this energy can be attributed to the ligation exchange (*18*). The β-branch reversion and closure restores about 6.6 kcal/mol relative stabilization of the reduced state.

c_1 (E_m = +240 mV) (*45*) possesses both the βXM motif and an extra loop with analogous cysteines (Figure 1). These cysteines are likely to be disulfide bridged since SDS gel electrophoresis of *Rba. sphaeroides* cytochrome c_1 is sensitive to reducing agent (*46*, *47*). Independence is supported by *Rhodospirillum rubrum* cytochrome c_1 (E_m = +320 mV) (*48*), which possesses the βXM motif but no loop.

Indeed, the βXM motif appears to be commonly associated with high midpoint potentials, not only in cytochromes c_1 (Figure 1) but also in mitochondrial soluble cytochromes *c* and bacterial cytochromes c_8. The position M *minus* 2 is almost exclusively occupied by the β-branched amino acid threonine in mitochondrial cytochromes *c* (*15*) and isoleucine or valine in cytochromes c_8 (*49*). A preliminary survey of the sequences approaching the heme ligating methionine suggests that restricted conformations of the β-branched amino acid in the βXM motif may be a common but certainly not the only means to maintain a tight environment around the heme to raise the potential in a rather large number of *c*-type cytochromes.

In 1994, Dolla et al. (*17*) concluded their analysis of the structural determinants of heme redox potentials in cytochromes *c* by considering how the "protein moiety" modulates the heme solvent exposure. By comparing structures of the class S, class M, and class L of bacterial cytochromes *c* described by Dickerson (*50*), they identified two ways that modulation of the heme exposure in monoheme cytochromes can be obtained. In the first, added loops decrease solvent exposure and raise the potential; in the second, contraction of the molecule, perhaps involving a hydrogen bond network around the heme (*16*), also increases the potential. Our site-

directed mutation and reversion experiments have documented the practical transformation of one distinct protein motif for modulation of the redox potential to high values into another. Disabling the disulfide bond anchoring the extra loop seems to sabotage the ability of this loop to insulate the heme from solvent exposure, lowering the midpoint in an example of Dolla's first strategy. The revertants, on the other hand, abandoned the first strategy for the second, by introducing a β branch to restrict the conformational flexibility around the heme. Such reduced flexibility could very well reduce the dynamic exposure of the heme to the solvent or "contract" the molecule. This was enough to raise the potential to a functional level, the same level (230 mV) as the βXM containing but loop-free mitochondrial cytochromes c_1. Interestingly, the βXM motif does not reduce heme solvent exposure or dielectric enough to obtain redox potentials above 300 mV. Native *Rba. capsulatus* cytochrome c_1 has apparently relied on the insulating ability of these extra loops to surpass the mitochondrial design and attain a potential of 320 mV.

The mutations we have described in *Rba. capsulatus* cytochrome c_1 reveal a potentially useful conformational plasticity of the sixth axial ligand domain. We anticipate that different mutations in this region can be introduced to modulate the redox potential without compromising assembly. Indeed, other cytochromes *c* may have naturally exploited the adaptability of this domain to develop other motifs besides the disulfide-anchored loop and βXM pattern to adjust the integrity of the heme-binding pocket and modulate the potential. Perhaps this is one of the reasons why no consensus sequence motifs are found in the location of the sixth ligand residue.

REFERENCES

1. Yu, C. A., and Yu, L., Eds. (1999) Cytochrome bc_1 complex, structure and function, in *J. Bioenerg. Biomembr.*, 167−288.
2. Berry, E. A., Guergova-Kuras, M., Huang, L., and Crofts, A. R. (2000) *Annu. Rev. Biochem. 69*, 1005−1075.
3. Dutton, P. L., Ohnishi, T., Darrouzet, E., Leonard, M. A., Sharp, R. E., Gibney, B. R., Daldal, F., and Moser, C. C. (2000) in *Coenzyme Q: Molecular Mechanisms in Health and Disease* (Kagan, V. E., and Quinn, P. J., Eds.) pp 65−82, CRC Press, Boca Raton, FL.
4. Li, Y., De Vries, S., Leonard, K., and Weiss, H. (1981) *FEBS Lett. 135*, 277−280.
5. Li, Y., Leonard, K., and Weiss, H. (1981) *Eur. J. Biochem. 116*, 199−205.
6. Gray, K. A., and Daldal, F. (1995) in *Anoxygenic Photosynthetic Bacteria* (Blankenship, R. E., Madigan, M. T., and Bauer, C. E., Eds.) pp 747−774, Kluwer Academic Publishers, Dordrecht, The Netherlands.
7. Brasseur, G., Saribas, A., and Daldal, F. (1996) *Biochim. Biophys. Acta 1275*, 61−69.
8. Xia, D., Yu, C. A., Kim, H., Xia, J. Z., Kachurin, A. M., Zhang, L., Yu, L., and Deisenhofer, J. (1997) *Science 277*, 60−66.
9. Iwata, S., Lee, J. W., Okada, K., Lee, J. K., Iwata, M., Rasmussen, B., Link, T. A., Ramaswamy, S., and Jap, B. K. (1998) *Science 281*, 64−71.
10. Zhang, Z., Huang, L., Shulmeister, V. M., Chi, Y. I., Kim, K. K., Hung, L. W., Crofts, A. R., Berry, E. A., and Kim, S. H. (1998) *Nature 392*, 677−684.
11. Hunte, C., Koepke, J., Lange, C., Robmanith, T., and Michel, H. (2000) *Structure 8*, 669−684.
12. Darrouzet, E., Moser, C. C., Dutton, P. L., and Daldal, F. (2001) *Trends Biochem. Sci. 26*, 445−451.
13. Stellwagen, E. (1978) *Nature 275*, 73−74.
14. Cusanovich, M. A., Meyer, T. E., and Tollin, G. (1988) in *Advances in inorganic biochemistry, heme proteins* (Eichhorn, G. L., and Marzilli, L. G., Eds.) pp 37−92, Elsevier, New York.
15. Moore, G. R., and Pettigrew, G. W. (1990) *Cytochromes c Evolutionary, Structural and Physicochemical Aspects*, Springer-Verlag, Berlin.
16. Caffrey, M. S., Daldal, F., Holden, H. M., and Cusanovich, M. A. (1991) *Biochemistry 30*, 4119−4125.
17. Dolla, A., Blanchard, L., Guerlesquin, F., and Bruschi, M. (1994) *Biochimie 76*, 471−479.
18. Tezcan, F. A., Winkler, J. R., and Gray, H. B. (1998) *J. Am. Chem. Soc. 120*, 13383−13388.
19. Springs, S. L., Bass, S. E., and McLendon, G. L. (2000) *Biochemistry 39*, 6075−6082.
20. Stonehuerner, J., O'Brien, P., Geren, L., Millett, F., Steidl, J., Yu, L., and Yu, C. A. (1985) *J. Biol. Chem. 260*, 5392−5398.
21. Tian, H., Sadowski, R., Zhang, L., Yu, C. A., Yu, L., Durham, B., and Millett, F. (2000) *J. Biol. Chem. 275*, 9587−9595.
22. Broger, C., Salardi, S., and Azzi, A. (1983) *Eur. J. Biochem. 131*, 349−352.
23. Atta-Asafo-Adjei, E., and Daldal, F. (1991) *Proc. Natl. Acad. Sci. U.S.A. 88*, 492−496.
24. Valkova-Valchanova, M. B., Saribas, A. S., Gibney, B. R., Dutton, P. L., and Daldal, F. (1998) *Biochemistry 37*, 16242−16251.
25. Laemmli, U. K. (1970) *Nature 227*, 680−685.
26. Thomas, P. E., Ryan, D., and Levin, W. (1976) *Anal. Biochem. 75*, 168−176.
27. Dutton, P. L. (1978) *Methods Enzymol. 54*, 411−435.
28. Goulding, C. W., Postigo, D., and Matthews, R. G. (1997) *Biochemistry 36*, 8082−8091.
29. Robertson, D. E., Ding, H., Chelminski, P. R., Slaughter, C., Hsu, J., Moomaw, C., Tokito, M., Daldal, F., and Dutton, P. L. (1993) *Biochemistry 32*, 1310−1317.
30. Gray, K. A., Davidson, E., and Daldal, F. (1992) *Biochemistry 31*, 11864−11873.
31. Matsumura, M., Signor, G., and Matthews, B. W. (1989) *Nature 342*, 291−293.
32. Betz, S. F., and Pielak, G. J. (1992) *Biochemistry 31*, 12337−12344.
33. Brems, D. N., Cass, R., and Stellwagen, E. (1982) *Biochemistry 21*, 1488−1493.
34. Carter, D. C., Melis, K. A., O'Donnell, S. E., Burgess, B. K., Furey, W. F., Jr., Wang, B. C., and Stout, C. D. (1985) *J. Mol. Biol. 184*, 279−295.
35. Klarskov, K., Van Driessche, G., Backers, K., Dumortier, C., Meyer, T. E., Tollin, G., Cusanovich, M. A., and Van Beeumen, J. J. (1998) *Biochemistry 37*, 5995−6002.
36. Klarskov, K., Verte, F., Van Driessche, G., Meyer, T. E., Cusanovich, M. A., and Van Beeumen, J. J. (1998) *Biochemistry 37*, 10555−10562.
37. Berghuis, A. M., Guillemette, J. G., McLendon, G., Sherman, F., Smith, M., and Brayer, G. M. (1994) *J. Mol. Biol. 236*, 786−799.
38. Qi, P. X., Beckman, R. A., and Wand, A. J. (1996) *Biochemistry 35*, 12275−12286.
39. Dumortier, C., Holt, J. M., Meyer, T. E., and Cusanovich, M. A. (1998) *J. Biol. Chem. 273*, 25647−25653.
40. Dumortier, C., Meyer, T. E., and Cusanovich, M. A. (1999) *Arch. Biochem. Biophys. 371*, 142−148.
41. Xu, Y., Mayne, L., and Englander, S. W. (1998) *Nat. Struct. Biol. 5*, 774−778.
42. Finnegan, M. G., Knaff, D. B., Qin, H., Gray, K. A., Daldal, F., Yu, L., Yu, C. A., Kleis-San Francisco, S., and Johnson, M. K. (1996) *Biochim. Biophys. Acta 1274*, 9−20.
43. Darrouzet, E., Mandaci, S., Li, J., Qin, H., Knaff, D. B., and Daldal, F. (1999) *Biochemistry 38*, 7908−7917.
44. Yeh, S. R., and Rousseau, D. L. (1998) *Nat. Struct. Biol. 5*, 222−228.
45. Andrews, K. M., Crofts, A. R., and Gennis, R. B. (1990) *Biochemistry 29*, 2645−2651.
46. Xiao, K., Yu, L., and Yu, C. A. (2000) *J. Biol. Chem. 275*, 38597−38604.

47. Konishi, K., Van Doren, S. R., Kramer, D. M., Crofts, A. R., and Gennis, R. B. (1991) *J. Biol. Chem 266*, 14270−14276.
48. Kriauciunas, A., Yu, L., Yu, C. A., Wynn, R. M., and Knaff, D. B. (1989) *Biochim. Biophys. Acta 976*, 70−76.
49. Ambler, R. P. (1996) *J. Mol. Evol. 42*, 617−630.
50. Dickerson, R. E. (1980) *Nature 283*, 210−212.
51. Shifman, J. M., Gibney, B. R., Sharp, R. E., and Dutton, P. L. (2000) *Biochemistry 39*, 14813−14821.
52. Fan, K., Akutsu, H., Kyogoku, Y., and Niki, K. (1990) *Biochemistry 29*, 2257−2263.
53. Dracheva, S. M., Drachev, L. A., Konstantinov, A. A., Semenov, A. Y., Skulachev, V. P., Arutjunjan, A. M., Shuvalov, V. A., and Zaberezhnaya, S. M. (1988) *Eur. J. Biochem. 171*, 253−264.
54. Dutton, P. L., Wilson, D. F., and Lee, C. P. (1970) *Biochemistry 9*, 5077−5082.
55. Pettigrew, G. W., Meyer, T. E., Bartsch, R. G., and Kamen, M. D. (1975) *Biochim. Biophys. Acta 430*, 197−208.

BI011630W